



Large-scale environmental sensing, e.g., understanding microbial processes in an aquatic ecosystem, requires coordination across a multidisciplinary team of experts working closely with a robotic sensing and sampling system. We describe a human-robot team that conducted an aquatic sampling campaign in Lake Fulmor, San Jacinto Mountains Reserve, California during three consecutive site visits (May 9–11, June 19–22, and August 28–31, 2006). The goal of the campaign was to study the behavior of phytoplankton in the lake and their relationship to the underlying physical, chemical, and biological parameters. Phytoplankton form the largest source of oxygen and the foundation of the food web in most aquatic ecosystems. The reported campaign consisted of three system deployments spanning four months. The robotic system consisted of two subsystems—NAMOS (networked aquatic microbial observing systems) comprised of a robotic boat and static buoys, and NIMS-RD (rapidly deployable networked infomechanical systems) comprised of an infrastructure-supported tethered robotic system capable of high-resolution sampling in a two-dimensional cross section (vertical plane) of the lake. The multidisciplinary human team consisted of 25 investigators from robotics, computer science, engineering, biology, and statistics. We describe the lake profiling campaign requirements, the robotic systems assisted by a human team to perform high fidelity sampling, and the sensing devices used during the campaign to observe several environmental parameters. We discuss measures taken to ensure system robustness and quality of the collected data. Finally, we present an analysis of the data collected by iteratively adapting our experiment design to the observations in the sampled environment. We conclude with the plans for future deployments. © 2007 Wiley Periodicals, Inc.

## 1. INTRODUCTION

Photosynthetic microorganisms contribute significantly to the base of the food web for freshwater and marine ecosystems. The growth of these planktonic microorganisms is dependent primarily on the availability of dissolved nutrients and light. Figure 1 displays a simple schematic representation of this interdependence. These variables display a high degree of variability in both time and space (Kratz, Deegan, Harmon & Lauenroth, 2003). As an illustration, the depth of light penetration into a water column is determined by the quantity and type of suspended particles, including inorganic materials (e.g., silts/clays), organic particles (decaying matter), and living organisms (bacteria, phytoplankton, and other microbes). Furthermore, nutrients (e.g., ammonium, phosphate) are generally removed from surface waters via uptake by phytoplankton, and are regenerated by decomposition that predominates in the deeper water. These regenerated nutrients are then made available to the surface-dwelling assemblages via vertical mixing of water. Phytoplankton often display maximum abundance at a certain depth [Figure 1(c)], an outcome of the higher growth rates adapted to optimize the availability of both sunlight and nutrients required for photosynthesis. As will be shown in this paper, this heterogeneity is typical for nearly all of the

observed variables in this environment. Understanding and predicting phytoplankton dynamics is dependent on characterizing such variables and other chemical and physical properties of the water column, as well as the interplay between the various taxa comprising the living community.

Given their highly dynamic nature, aquatic ecosystems have traditionally remained undersampled, both temporally and spatially, because of the difficulties and the associated cost of continuously accessing these environments (Gelda & Effler, 2002b; Lopez-Archilla, Molla, Coletto, Guerrero & Montes, 2004). Our understanding of how these communities are composed and function has been constrained by our limited knowledge of processes taking place on spatiotemporal scales not typically captured by traditional sampling approaches. For these reasons, studies of aquatic microbiology are highly suited for the application of embedded sensing networks that can provide synoptic spatial coverage as well as high temporal resolution of pertinent environmental features. We use the term “campaign” to refer to a set of field experiments performed with several robotic sensing devices over a span of a few days and spread over several months, with an objective of performing detailed characterization of phenomena of interest.

In this paper we describe an aquatic monitoring campaign performed by a human-robot team from

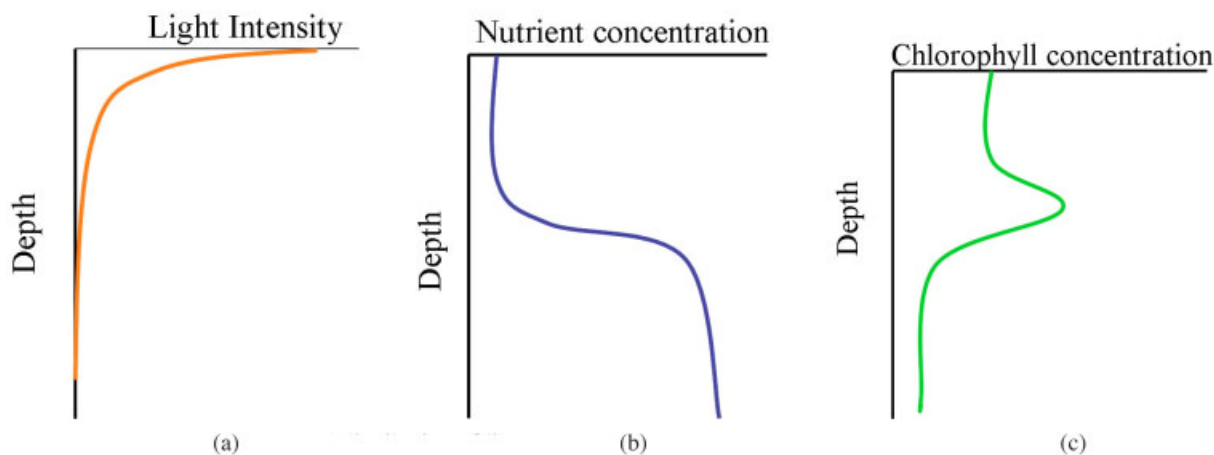


**Figure 1.** Interdependence of environmental conditions and growth of phytoplankton. (a) Expected distribution of light intensity. (b) Expected distribution of nutrient concentration. (c) Expected distribution of phytoplankton (correlated with expected concentration of chlorophyll).

the University of California Los Angeles and the University of Southern California. The goal of this study was to establish, test, and employ a suite of static and mobile sensor technologies in a small lake, Lake Fulmor (James San Jacinto Mountain Reserve, 2006), in order to enable biological studies of the phytoplankton community. A satellite view of the lake is shown in Figure 2. It has a single source of freshwater at its northern end and a single outlet at its southern end. Flow into and out of the lake nearly ceases during much of the summer/fall period, making it an excellent model system for studying phytoplankton dynamics in the absence of large advective processes.

The campaign reported herein includes three consecutive system deployments (May 9–11, June 19–22, and August 28–31, 2006), spanning over four months and involving 15 to 25 investigators from multiple disciplines (robotics, engineering, computer science, statistics, and biology). The deployed system consisted of both static and mobile sampling systems. The networked aquatic microbial observing systems (NAMOS) consisted of five to eight buoys (depending on the deployment) and a robotic boat. The buoys provided continuous measurements of the observed parameters at different depths over statically distributed locations across the lake. The boat provided the surface measurement of the observed phenomena across the lake environment. An infrastructure-supported tethered robotic system, Rapidly Deployable Networked InfoMechanical Systems (NIMS

(Jordan, Batalin & Kaiser 2007) (hereafter called NIMS) was used to navigate a sensor payload anywhere within a two-dimensional cross section (vertical plane) of the lake system. Thus, together such an array of robotic sampling systems enables a near-complete three-dimensional characterization of the lake environment.

Each of these systems is equipped with an array of sensing elements for documenting the physical and chemical structure of the lake. This enables the characterization of the spatial and the temporal changes in the parameters affecting the growth of phytoplankton (temperature, fluorescence, dissolved oxygen, pH, etc.). To ensure the correctness of the collected data, and hence the system robustness, data collected after each experiment were analyzed in-field by the multidisciplinary team of experts. Based on this analysis, a decision was taken to either repeat a specific experiment to ensure the integrity of the collected data or to adapt the next set of experiments to validate the known understanding and newly developed insights (based on the analysis from previously conducted experiments) about the observed environment. This enabled the collection of increasingly relevant data for future measurements.

This teamwork paradigm involved implicit coordination between the sensing systems through the explicit interaction with the human experts in the loop while the field campaign is underway. Large team efforts and uncertainties associated with operation in



**Figure 2.** Satellite view of Lake Fulmor, a small (1.2 hectare) lake located in a subalpine (1600 m), coniferous forest within the San Jacinto mountains of Southern California.

the real world scenario constrains the field campaign time to a short duration. An explicit interaction with the human experts who analyze the collected data in-field results in efficient use of this limited field campaign time.

Such an interaction between human experts and robotic systems occur at several levels: first, the sensing/robotic system is tasked with a particular sampling algorithm to collect the data; second, the data are analyzed by the team of human experts to decide the next set of sampling experiments to be performed; third, the sampling design is adjusted appropriately on each robotic or stationary sensing element to capture the desired field variable for effectively characterizing the spatiotemporal distribution of the observed environment. Based on our experiences with other field campaigns in the past (Harmon et al., 2006; Singh et al., 2007a), having such teamwork with human experts in the loop to analyze the observed variables in-field and to adapt the experimental design accordingly ensures that the integrity of the collected data is reliable.

Monitoring of physical phenomena in an ecosystem with largely unknown spatiotemporal dynamics and biological characteristics was greatly benefited by the presence of a multidisciplinary team. Each member performed a specific role, contributing to the

successful completion of the campaign. The biologists provided the motivation for the campaign and performed analysis of the water samples collected manually or by actuating NIMS to collect samples from precise depths within the sampled cross section. Together with the statistics experts, who provided data representation and feature extraction for the observed variables, they performed biological interpretation for the collected data. Computer scientists designed and implemented the control algorithms for the NAMOS and NIMS systems, real-time data collection and management, as well as in-field modifications to the control code required to accurately capture the biological features, previously unknown and discovered in the previous experiments. Finally, engineers maintained the electromechanical components and performed regular maintenance and recalibration of the systems to ensure high fidelity and integrity of the collected data.

## 2. CAMPAIGN REQUIREMENTS

A typical environment sensing campaign, such as an assessment of the relationship between water quality characteristics within a lake and the resulting biomass and species composition of the phytoplankton

assemblage, would require detailed observation in four dimensions (three dimensions in space and one in time) over time scales ranging from hours to seasons. Such a characterization would help scientists to better understand the observed phenomena, its correlation with the observed variables, and the development of new hypotheses based on the observations made during the field campaign.

Obtaining such a characterization of both spatial and temporal dynamics imposes constraints on the design and development of the sensing system used for making observations. It is presumably hard to develop a single system capable of addressing all scales of measurement that are necessary for fully characterizing and predicting the spatiotemporal dynamics in a natural ecosystem. Thus, it is important to define a specific objective or objectives for each study and to design the appropriate suite of robotic and sensor systems for the corresponding objective(s). A static sensing system can be used to provide information across temporal scales ranging from seconds to days. On the other hand, mobile robotic systems can provide information on the three-dimensional spatial distributions of biological, chemical, and physical parameters over scales ranging from centimeters to tens of meters. Thus, a combination of static and mobile sensing devices is better suited to satisfy the requirements of high fidelity characterization of spatiotemporal dynamics associated with environmental sensing applications. Repeated visits to the study site are required to further acquire information across seasons.

Combining mobile robotic systems with an array of static sensors, the characteristics of the environmental medium can be resolved at a higher rate and with a spatial resolution greater than in previous investigations (Gelda & Effler, 2002b; Lopez-Archilla et al., 2004). A challenge typically associated with environmental sensing campaigns is incomplete knowledge of the phenomena under study. This necessitates an in-field analysis of the observed data and adaptation of the experimental design accordingly.

Efficient field characterization with a combination of static and mobile sensing devices further involves a two-tier deployment approach: (1) A first stage campaign where at a relatively low cost, a static distributed sensing system is deployed at multiple locations and times providing evidence regarding phenomena distribution information at a sparse temporal scale, such as an annual cycle, followed by (2) a second stage of deployment where the mobile robotic

systems are deployed at the locations and times identified through analysis of the first stage observation. During each stage, careful experiments need to be designed that may guide the deployment and redeployment of these systems for the purpose of optimizing characterization fidelity and to address the requirement of high spatiotemporal resolution sampling. These characteristics require a possible in-field adaptation of the measurement system to allow optimal operation in the presence of rapidly evolving environmental features. Thus, an iterative experiment design approach—adapting the next set of experiments based on prior understanding and current observations from previous experiments, is required to guide the autonomous operations of mobile sensing devices.

Specific application requirements guide the sampling rate for both static and mobile sensing devices and sampling density for mobile robotic systems. In the absence of experiments that previously had been executed in a given environment, these parameters are initialized based on the expert opinion of application scientists. These parameters can then be iteratively improved upon based on observations from field experiments. Other system parameters such as speed of the mobile robotic systems need to be designed so as to address the specific spatial and temporal sampling requirements of the application as well as to ensure that the sensing system does not interfere with the phenomena under observation.

### 3. SYSTEM DESCRIPTION

Collectively, the NIMS and NAMOS systems permit various configurations of sampling. NIMS is an actuated cable-driven robot, while NAMOS is composed of a set of static buoys and a robotic boat. In the experiments described in this article, we anchored a set of buoys at pre-determined positions [selected by the biologists on the team for low resolution spatial sampling but high temporal resolution sampling, as shown in Figure 3(a)]. Measurements of temperature and fluorometry (a proxy for chlorophyll concentration) were obtained from these buoys throughout the campaign. Based on the data analysis from previous buoy deployments during 2005, NIMS was deployed across the lake at a position that was most likely to provide characterization of a representative area within the lake. NIMS navigates the sensor payload, described in Section 3.2.4, anywhere within the se-

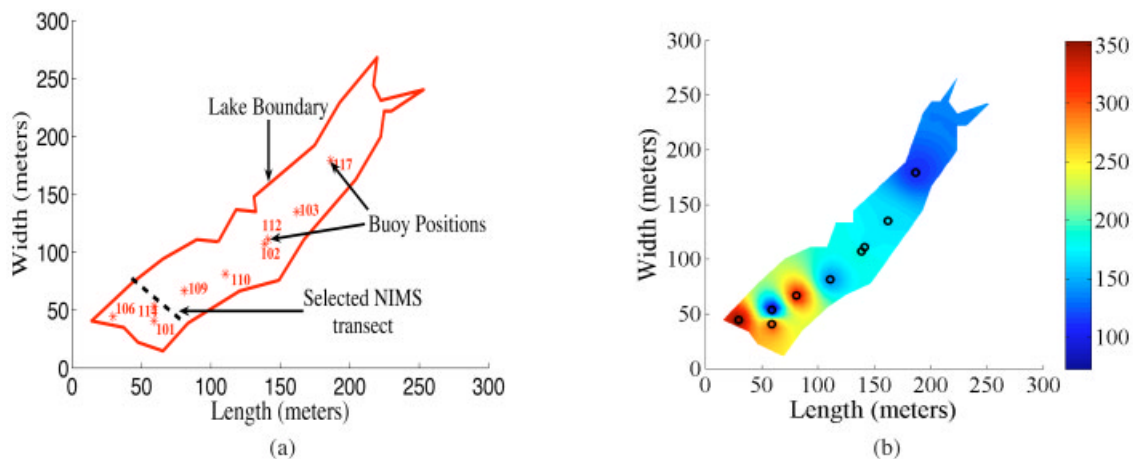


**Figure 3.** Static buoy positions and corresponding snapshot of sampled chlorophyll concentration (depth=0.5 m) during the August part of the campaign. (a) Location of static buoys during Aug. 28-Aug. 31. (b) Chlorophyll distribution (micrograms per liter) at 9:46 a.m., August 31, 2006.

lected vertical plane. The navigable sensor node is actuated throughout the span of the vertical plane in several modes: point sampling, deterministic raster scanning following a “comb” pattern (hereafter referred to as raster scan) and data-driven adaptive sampling approaches. In the course of other experiments we have used samples from the buoys to guide the sampling schedule of the robotic boat, as will be reported in future publications.

### 3.1. NAMOS: Buoys and Robotic Boat

NAMOS is a sensor-actuator network for freshwater and marine monitoring (Sukhatme et al., 2006). The system consists of ten static sensor nodes (buoys) and one boat, as shown in Figure 4. For the purpose of this campaign, the boat was used as a standalone system only. The boat was simply used for data collection experiments to contribute to a detailed characterization of the environment.

Each buoy, as shown in Figure 4(b), is enclosed in a 113 l, 45 cm diameter  $\times$  75 cm tall, high density polyethylene drum with a flat lid bolted on top. There is a tire inner tube fit midway around the drum to provide stability. All internal components are mounted on a removable inner chassis. At the bottom is a sealed 108 A h 12 V rechargeable battery. A low power embedded system, Stargate,<sup>1</sup> support-

ing an embedded Linux operating system, provides data logging, subsystem control, and wireless communication via 802.11b. For the purpose of this campaign, communication between the buoys is limited to relaying the collected data to the base station and synchronizing the clocks on each system such that the collected data can be merged accurately with the data from other systems.

Data capture is accomplished by a custom built eight-channel, 12-bit and single-channel, 16-bit analog to digital conversion (ADC) system. Since data are logged internally, and each of the buoys could potentially be placed at a distance of more than 300 m from the central base station (where experts are analyzing the data in real-time), the communication to the outside environment is preferable using a wireless connection. All buoys have a string of six thermistors for temperature sensing that can be adjusted to different depths. Six buoys have a large area photodiode for approximation of solar radiation. A Cyclops-7 fluorometer<sup>2</sup> is also included on each buoy. One of the buoys also includes a wind vane and anemometer for wind direction and velocity.<sup>3</sup> Another buoy, outfitted as a weather station, is set up on land. Sensors for this buoy include wind direction and velocity, humidity, air tempera-

<sup>1</sup>Developed by CrossBow Technology.

<sup>2</sup>Developed by Turner Designs.

<sup>3</sup>Developed by Texas Elelectronics.



**Figure 4.** NAMOS components. (a) System of buoy and boat deployed during the campaign. (b) Detailed system description of a buoy.

ture, rain, barometric pressure,<sup>4</sup> and a quantum photo synthetically active radiation sensor.<sup>5</sup>

The software running on each buoy is built on the EmStar runtime environment (Girod et al., 2004), a software system for developing and deploying wireless sensor networks on Linux-based platforms. The buoys are configured to run in ad-hoc mode. A multihop protocol is used to create a dynamic routing tree that can reliably route packets through the network. The software on the buoys consists of three different modules: (1) an ADC module to sample the sensor data; (2) a storage and communication module to log the sampled data to a local disk storage and to transmit it to the base station on the shore; (3) a time-synchronization module providing the essential accurate time stamp for sampled data as required for analysis. The ADC module running on the weather station is a modified version of the previous as it incorporates additional computation for converting the voltage readings for various sensors into their corresponding standardized units (e.g., mph for wind speed, mm for air pressure, etc.).

The robotic boat is a modified radio-controlled air boat. The boat is designed to primarily operate in small lakes and ponds with negligible water flow. The small size (about 3 ft in length) of the boat makes it susceptible to wind and wave action,

<sup>4</sup>Developed by Texas Elextronics.

<sup>5</sup>Li-Cor, developed by Glen Spectra.

thereby rendering it unsuitable for ocean and river-like environments. An air propeller provides propulsion and minimizes disturbance to the water caused by the movement of the boat, which is important for the biology study. The boat is also equipped with a global positioning system (GPS) and compass module for navigation. The GPS on the boat has an accuracy of less than 15 m (95% typical) with an update rate of 1 s propagated every 200 ms. During this campaign, the GPS was used in Wide Area Augmentation System (WAAS) enabled mode that provided a positioning accuracy between 6–8 m. The compass has an accuracy and resolution of 0.1°. The sensor suite on the boat consists of a thermistor and a fluorometer. Communication with the boat takes place via an 802.11b wireless connection. The boat is powered using rechargeable NiMH batteries, which at present provide an approximate lifetime of 4–6 hours of continuous operation.

The boat can operate in two modes. In the human guided mode, a human operator can give the commands to the boat (left, right, forward, reverse, stop, sample) using a joystick controller. In the autonomous mode, the boat can be given a trajectory to follow in terms of GPS waypoints (latitude and longitude combinations). The boat can use its onboard GPS and compass to plan the path to reach the specified target points in that order. Currently, we do not have any camera, laser, or sonar on the boat to give

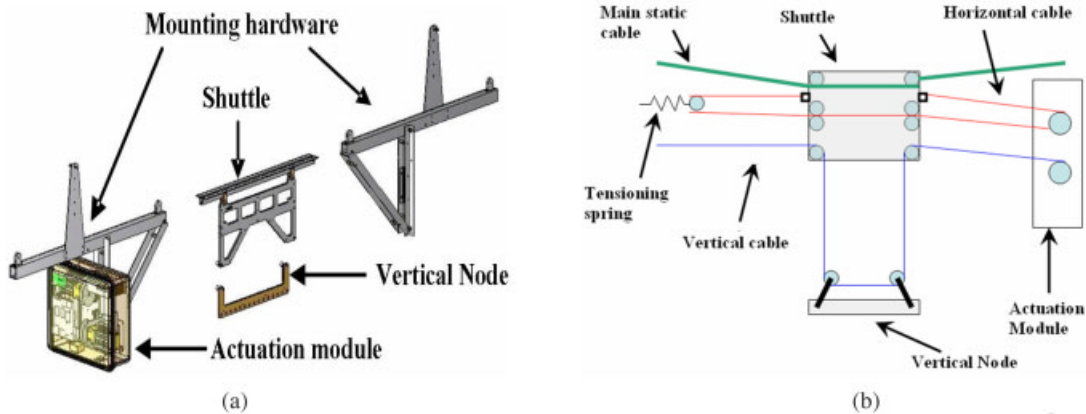


**Figure 5.** NIMS: Schematic design. (a) Major components of the system without the cable infrastructure. It also shows the relative layout and orientation of the system, although they would be much more spread out in reality. (b) Schematic view with the basic cable setup.

enough information to the boat to detect and avoid obstacles. This is part of our ongoing work on a new bigger, more capable boat.

### 3.2. NIMS: Rapidly Deployable Cabled Mobile Platform

NIMS is an infrastructure-supported tethered robotic system capable of precise positioning within a vertical plane along its span (schematic description shown in Figure 5). A description of the hardware systems and software architecture is explained in the following sections.

#### 3.2.1. System Description

NIMS consists of three main cables: the mounting hardware, actuation module, and shuttle and vertical platform. The three cables are a static cable used to support the complete system and horizontal and vertical cables used to control the corresponding motion of the sensor payload. The static cable can be attached via ground anchors and routed over a support stand or anchored to any suitably strong structure (e.g., trees, railing, poles, etc.). The primary static cable used in our campaign is a  $7 \times 19$  class strand core, nylon coated  $3/16$  in. wire rope rated at 1760 lbs break strength.<sup>6</sup> Since the primary cable is never subjected to shock loads, a precautionary limit

<sup>6</sup>Produced by McMaster-Carr.

is set to stay at 50% or lower of the break strength of the cable ( $\leq 880$  lbs). The mounting hardware is supported by the static cable and is used to attach the actuation module on one side and horizontal and vertical cables return on the other side. Please refer to Figure 5(a) for a graphical representation of the description. The actuation module contains two motors that spool the horizontal and the vertical cables in or out resulting in the two-dimensional actuation of the sensor payload within the vertical plane. When the diameter of the spools are factored in, this results in a maximum payload support of 13–30.3 kg, a maximum vertical speed between 2 and 4.7 m/s, and a maximum horizontal speed of 6.7 m/s.

The sensor box, shown in Figure 6(a), is attached to the shuttle and consists of a pelican case outfitted with a variety of bulkhead connectors. It houses the serial-ethernet bridge, the ethernet-copperlink converter, a relay control board, and several AC/DC power supplies. It includes a single AC input power connector, one ethernet input, and several serial outputs for each of the attached sensor and power outputs that can be easily configured as per the requirements. The case is watertight; however, two apertures are added at the bottom of the case to allow for the addition of cooling fans. A rectangular aperture is also necessary in the back to allow for the cables to exit. This access for cable actuation is outfitted with dual brush systems that block the opening against contamination as well as clean the cables

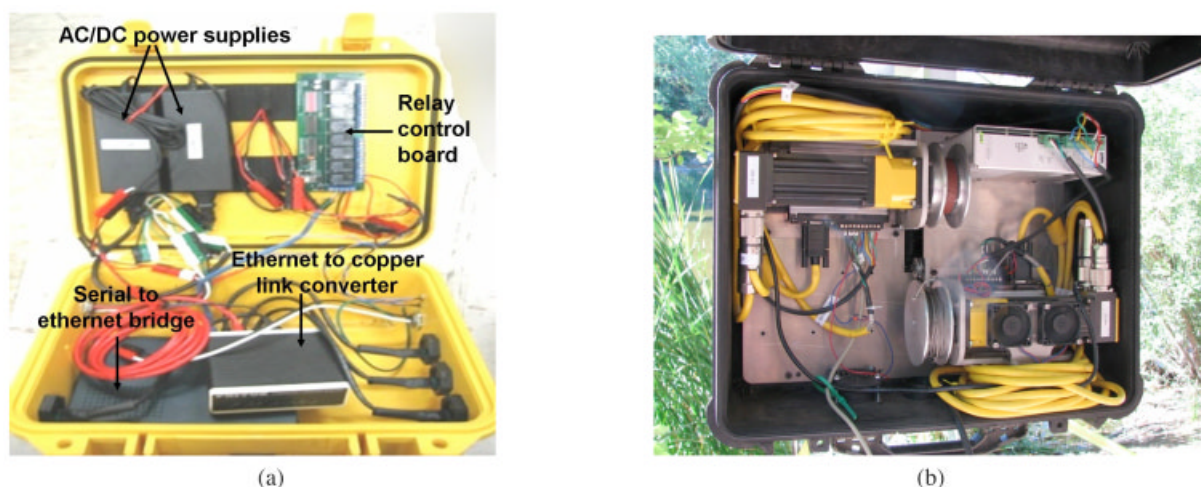


**Figure 6.** NIMS: System components. (a) Sensor box attached with the shuttle. (b) Motor system actuating the mobile robot.

as they enter. This case, although not watertight, is extremely weather resistant and allows the system to withstand wet and rainy conditions (this NIMS RD system has operated in a rainforest environment in Costa Rica for forest ecosystem studies).

Current NIMS design has improved upon the previous NIMS systems (Pon et al., 2005) in substantially reducing the limitations for rapid and flexible, short-term deployment. It retains the infrastructure and mass support cableway of the previous NIMS systems, which provide low energy and position-accurate transport. This new system is able to provide precise position control (millimeter resolution) and is easily transportable. In 2006 alone, NIMS was used in several successful campaigns in forests (La Selva, Costa Rica, and James Reserve, California), rivers (San Joaquin River, California, and Medea Creek, California), a lake (Lake Fulmor, California), and mountains (White Mountains, California), varying in spans from 5–90 m.

### 3.2.2. Software Architecture

NIMS is controlled using an interactive Python application running on a laptop that is in constant communication with the motor system via RS-232 interface. The main application has two modes of operation:

1. User interactive via menu: Allows the user to freely control the movement of the robotic

system using regular keyboard control. This mode is primarily used for calibration, sounding, and point movement for collecting physical water samples.

2. Feedback based control: Provides feedback from the system to the end user (controlling application) when a set of desired locations is visited. This allows the interacting application to visit a set of locations to observe prior to making a decision on the next location (or a set of locations) to visit. It is also possible to get a real-time display of the observed data as collected by the sensor payload in this mode.

NIMS uses an anchorless coordinate system that allows the user to set an arbitrary point in the vertical plane as the origin. This is achieved by calibrating the motor resolver readings to real physical locations. During our campaign, we designated  $x$ -axis along the cross section of the lake and  $y$ -axis along the depth. Zero for the  $y$ -axis was set to be at the surface. The  $x$ -values are related to an independent calibration cable that runs parallel to the primary cable just above the path of shuttle travel. The calibration cable is kept under tension such that there is minimal deflection (less than  $1^\circ$ ) from the horizontal. Markers, placed at known distances (at every 5 m separation), are used to calibrate the system in an effort to provide accurate localization. For calibration, motor positions for a set of known marker lo-



**Figure 7.** NIMS: Pictures from the campaign describing several components. (a) Field snapshot of sampling using NIMS. (b) Image taken during the campaign.

cations (typically five to ten positions) are recorded and a polynomial fit is performed to interpolate for the intermediate positions and account for the parabolic drift in the horizontal cable due to the weight of the system. The system itself assumes that no obstacle is present on the way when it is directed to move from one location to another. However, any obstacle avoidance approach can be easily integrated along with the end user (control) application to result in obstacle free path planning.

### 3.2.3. Data Collection and Power: Modularity and Scalability

Sampled data from the sensor payload attached to NIMS were observed in real-time to validate accurate sampling and detect system errors if and when they might occur. Modularity, scalability, and robustness were a few of the important considerations while deciding how to route the data back to the shore where they could be analyzed for possible errors. Each of the sensors communicates over RS-232 serial interfaces (which has a physical limitation in terms of maximum transmission distance less than the length of the NIMS transect). NIMS required the ability to scale data transmission to longer transects and to support multiple sensors using a single link. A serial-ethernet bridge was used on the system, which supports four input serial channels, and is optionally upgradeable to 16 channels without any change in the software. This provided multiplexed

output on a single ethernet output link, which was then converted using an ethernet to the copper link converter, thereby increasing the maximum possible transmission length to approximately 1300 m. Figure 7(a) shows the data festooning used for this purpose. On the shore end, copper link is converted back into the ethernet. Data from individual serial channels are retrieved from the ethernet link connected to the laptop. A direct data link without any bandwidth constraints to the shore side also resulted in avoiding the requirement of an embedded platform on the system for data preprocessing prior to transmission.

Many typical aquatic sensor systems carried as payload may not always be capable of operating using only internal batteries for the required operating lifetime. Typically, devices and sensors require a variety of input voltages and routing DC power over 500 ft of cable proved to be very inefficient due to a relatively large voltage drop. To accommodate different power requirements while still providing robustness and scalability, we routed 110 V AC that was supplied by batteries on shore to the mobile system via the festooning, as shown in Figure 7(a).

### 3.2.4. Sensing Systems

The NIMS system utilizes two water quality probes from Hach Environmental:<sup>7</sup> the Datasonde model DS5 and the Datasonde model 4a. Each of these

<sup>7</sup>Developed by Hach Environmental.

probes is equipped with a suite of sensors and is capable of internal data logging in addition to real-time data streaming. When logging internally, the maximum sampling rate is 0.1 Hz while with real-time data streaming the maximum sampling rate is 1 Hz. Each probe can be powered with internal batteries or externally via DC power. For the May and June parts of the campaign, data were collected using the internal logging mode and the probes were battery powered. During the August part of the campaign, both internal logging and real-time data streaming were employed but power was again provided by the batteries. The DS5 model contains eight different sensors for observing temperature, pH, oxidation potential, specific conductivity, depth, photosynthetically active radiation, turbidity, and dissolved oxygen. The 4a model contains five different sensors: temperature, pH, conductivity, nitrate ( $\text{NO}_3^-$ ), and ammonia ( $\text{NH}_4^+$ ).

For the deployments in May and June, with sensors programmed to internally log data at a 0.1 Hz, a dwelling time of 15 s was chosen for each observation location to ensure that at least one sampled datum is logged for each position. For the deployment in August, real-time data was recorded (using the festooning cable) at 1 Hz and simultaneously merged with the positional data from NIMS. Since the data were collected every second, the dwelling time at each position was reduced to 10 s. This also enabled several readings from each position that helped in analyzing short-term temporal variation and characterizing the response time of the sensors.

Chlorophyll sensing on the NIMS is achieved by use of a Cyclops-7 fluorometer,<sup>8</sup> calibrated for chlorophyll-a. This is connected to a waterproof enclosure containing electronics for voltage regulation, ADC, and RS-485 serial data transmission. Both the supplied power and the collected data are transmitted by a festooned Cat5 8-conductor cable. At the shore, three 6 V sealed rechargeable batteries in series provide power. Data is converted from RS-485 to RS-232 for connection to a laptop for logging.

The physical sampling device was designed and developed by our team for collecting physical samples of water at any position. It uses dual spring-loaded syringes capable of collecting a combined 80 ml of fluid. A linear solenoid actuator combined with relay switching enables a trigger mechanism where the spring-loaded syringe mechanism oper-

ates, drawing a water sample. After transfer of water samples to a canister at the shoreline, the sampling system is prepared for a next sample by deflecting the springs in preparation for future solenoid trigger events. Figure 8 shows the collection of this sensor suite used during the campaign.

### 3.2.5. System Robustness

Robust characteristics have been introduced into the NIMS system for both operation and data acquisition. A dynamo meter was placed in line with the primary cableway in order to verify that the system stayed within the safety bounds of the cable. Currently, the tension is monitored manually by the operator of the system; however, plans are underway to automate this procedure and make cable tension part of the feedback control for the system.

The sensor payload consisted of both the Hydro-lab probes to provide redundant sources of input. Each probe is capable of accepting external power as well as relying on internal battery power. This provides protection against data loss in the case of interruption in external power supply. During the deployment in August, one of the sensor systems displayed failure in serial port communication during a scan. Redundancy in the sensor suite ensured that sampling remained possible for the rest of the scan (and the rest of the deployment). An additional redundancy is introduced in the data capture by applying both real-time monitoring (relying on data transmission cables) as well as the simultaneous archiving of data within the sensor systems using their internal nonvolatile memory storage. Thus, in the event of data transmission errors or failures, data still remain available. A similar approach was used for the physical sampling system. In order to guarantee a minimum of 20–30 ml samples per location (a typical requirement for conducting several biological experiments) a dual 50 ml syringe sampler was built. By having a dual syringe sampler it is possible to extract 70–80 ml of sample from each location and in the case of a misfire, a single syringe is capable of extracting 35–40 ml that is sufficient for the analysis by the biology team.

## 4. EXPERIMENTAL DESIGN AND ANALYSIS

Experiments were designed carefully using the available robotic sensing systems and were iteratively im-

<sup>8</sup>Developed by Turner Designs.

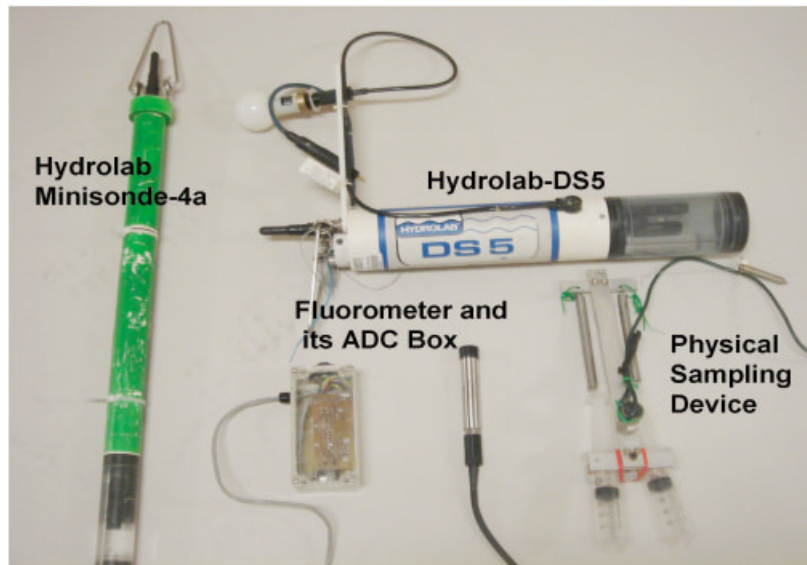


**Figure 8.** Sensor payload carried by NIMS during the campaign: (1) Hydrolab Datasonde model 4a measuring temperature, pH and specific conductivity (2) Hydrolab Datasonde model DS5 measuring depth, oxidation reduction potential, turbidity and luminescent dissolved oxygen (3) Fluorometer measuring fluorescence (proxy for the concentration of chlorophyll-a) (4) Physical sampling device, developed by our team for collecting water samples.

proved over the subsequent campaigns. This enabled high-fidelity characterization of the lake environment. Static buoys were distributed over the entire lake to provide high temporal resolution data at several point locations. NAMOS boat was used to perform the surface scan, measuring both temperature and fluorescence. Such experiments performed at earlier stages of the campaign enabled the selection of a particular transect, along the cross section of the lake, wherein NIMS performed high-resolution sensing experiments. The total length of the transect along the cross section of the lake was 45 m and the depth was up to 4.5 m. Observations made during such experiments are discussed later in the section. Whenever multiple observations were taken at a single location (a “dwell point”) by the robotic unit, the mean value is used as an observation from that location. Only a small subset of observed variables that was representative of distribution exhibited by other observed parameters is displayed in this paper. In what follows, our surface displays are constructed from simple bilinear interpolation. This did not introduce any detectable artifacts, although other kinds of smoothing (estimation rather than interpolation) might be more appropriate for noisy data.

#### 4.1. Iterative Experiment Design

This campaign demonstrated the successful application of the iterative experiment design for environment applications (IDEA). A detailed description and the usefulness of such an approach are addressed using experiences from another field campaign involving NIMS (Singh et al., 2007b). This approach ensures detailed characterization of an environment where the observed parameters and their interrelation is widely unknown. Dense spatial sampling is performed to characterize the spatial distribution of the observed variables with high fidelity. Sampling density for such scans is iteratively improved in consultation with the application domain experts. This resulted in increased sampling density in the vertical direction from observation locations separated by 50 cm during the deployments in May and June to observation locations separated by 15 cm during the deployment in August.

Such scans were then repeated during different times of the day to characterize the diurnal variation in the observed variables. In addition to providing temporal variation in phenomena characteristics, these scans also provided periodic sampling checks

for postdeployment calibration, data integrity, etc., and a baseline to characterize the performance of any adaptive sampling approach. Dwelling time at each observation location, while performing raster scans, was selected so as to satisfy both the requirements for observing short-term temporal variations across the complete observed environment and the response time of the sensing system. This dwelling time was also iteratively improved from 30 s during the deployments in May and June to 10 s during the deployment in August based on expert analysis of the collected data and improvement in the system capabilities (real-time data logging from the sensors increased the sampling rate from 0.1 Hz to 1 Hz, as discussed in Section 3.2.4.).

Finally, based on observations from the collected data, experiments were designed to characterize the constraints of the sampling system, such as localization drift, interference in the observed environment, and others, such that the integrity of the collected data can be established. These involve using the depth sensor to validate the localization provided by the actuator system, and adaptive experiments to characterize the mixing of water by vertical motion of NIMS inside the water, among others.

#### 4.2. Temporal Trends

Static buoys containing fluorometer for sensing chlorophyll-a at the depth of 0.5 m and temperature at six depths (0.15, 0.65, 1.15, 1.65, 2.15, and 2.65 m) were deployed at spatially sparse locations to understand the spatial variation in phytoplankton distribution across the lake and to record high-resolution temporal data. Locations chosen for the campaign during August are shown in Figure 3(a). Figures 9(a) and 9(b) display the temperature and the fluorometric data respectively, collected from one of the buoys during the two deployments. Data were collected at the rate of 1 measurement/s for several days. Significant diurnal variation in temperature at different depths and chlorophyll-a concentration at a depth level of 0.5 m was apparent. The depth for the fluorometer was chosen to represent phytoplankton abundance in the surface mixed layer (Figure 1). A specific structure in the diurnal variation can be easily observed in the fluorometer data with a minimum occurring around noon everyday. Figures 9(c) and 9(d) display the variation in the maximum and the minimum temperature recorded by the buoys during the three campaigns at different depths.

Significant vertical, diurnal, and seasonal variations in temperature were apparent at all depths examined. Diurnal temperature changes during each sampling period were greatest for surface waters, as would be expected for the high light intensities experienced by this subalpine lake.

#### 4.3. Spatial Trends

In addition to the data from the static buoys, the NAMOS boat was used to perform surface characterization of the lake during the deployment in May. GPS readings were recorded along the path followed by the boat while sampling the temperature and the fluorometer data. It took approximately an hour to perform dense sampling at the surface of the lake. Figure 10(a) displays the distribution of sampling locations, with a total of 1075 locations sampled along the followed path. Local linear regression was applied to the sampled data and the smoothed temperature distribution on the surface of the lake is demonstrated in Figure 10(b). It is easily observed that there was negligible (approximately 1 °C) temperature variation between the sampled locations on the surface, compared to considerable temperature variation along the depth, as shown in Figure 9(a).

Using the data from the coarse spatial distribution of the buoys, combined with the surface phenomena distribution provided by NAMOS boat, several candidate locations for the NIMS transect were chosen to provide a high-resolution spatial map at a cross section of the lake. Within one such selected cross section [see Figure 3(a) for reference], NIMS was used to navigate the sensor payload (described in detail in Section 3.2.4.). During the campaigns in May and June, the sampling design was taken to be a grid with points spaced every 2 m along the transect and at every 0.5 m of depth. This resulted in a set of 197 sampling locations that were visited approximately every 2 h over the course of almost two days. This sampling density was decided in consultation with the biology experts in our team. With dwelling time at each location fixed to 15 seconds, the total sampling time was around 1 h and 30 min for the complete raster scan. Autonomous raster scans, one after the other, were performed during these two deployments to get diurnal variations in the sampled phenomena along with its high spatial resolution characterization.

Analysis of the data from the two campaigns in May and June influenced the experimental design

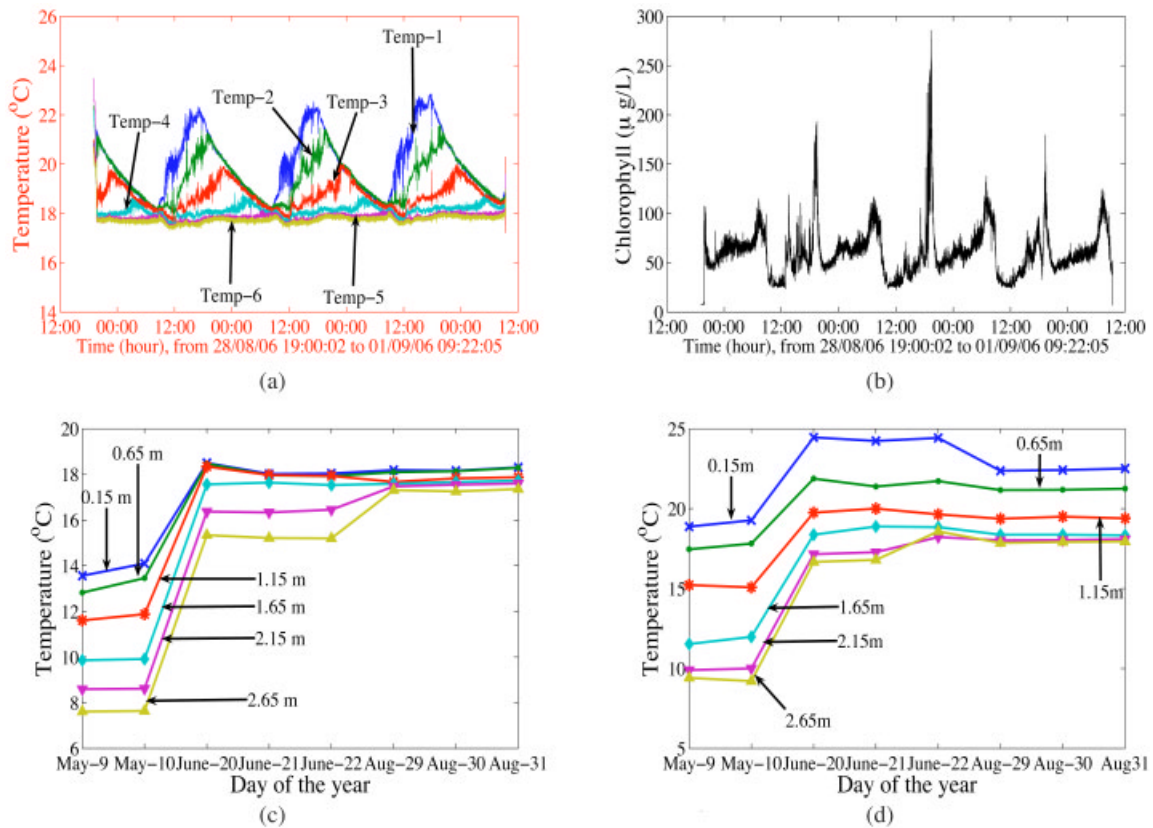


**Figure 9.** Analysis of diurnal and seasonal variation in temperature distribution during the campaign: The six thermistors were at depths of 0.15, 0.65, 1.15, 1.65, 2.15, and 2.65 m, respectively. The fluorometer was at the surface of the water. (a) Temperature data from one of the buoys during August deployment. (b) Corresponding fluorometer data from the same buoy during August deployment. (c) Variation in minimum temperature recorded by the buoys during the three campaigns. (d) Variation in maximum temperature recorded by the buoys during the three campaigns.

during the deployment in August. In turn, the biology underlying the fluorometry readings, illustrated in Figure 1 and discussed in Section 1, responds at least in part by displaying the peak at subsurface level along with another smaller peak at a deeper level, which is not clearly understood. This is in conformance to the temperature stratification as well as the spatial distribution of the light conditions and the available nutrients in the lake. To further investigate the spatial patterns with high resolution, the sampling density along the depth was decreased to 0.15 m, keeping the sampling density along the cross section fixed at 2 m. This resulted in a total of 732 sampling locations for the complete raster scan. With the increased resolution, an issue that needs to be resolved is whether vertical motion of the NIMS

node is causing any interference in the sampled environment by churning the water from different strata. We designed two experiments to understand this effect. Detailed analysis from these experiments is presented in Section 4.3.1. During the August campaign, with increased sampling frequency of 1 Hz, dwelling time at each location was reduced to 10 s, providing 10 consecutive observations at each observation location. Sampling time increased to approximately 3 h for the complete raster scan after increasing the sampling density to 732 locations. Four such scans at different times of the day were performed over the period of three days during this deployment.

Spatial distribution for temperature and dissolved oxygen as observed during one of the raster

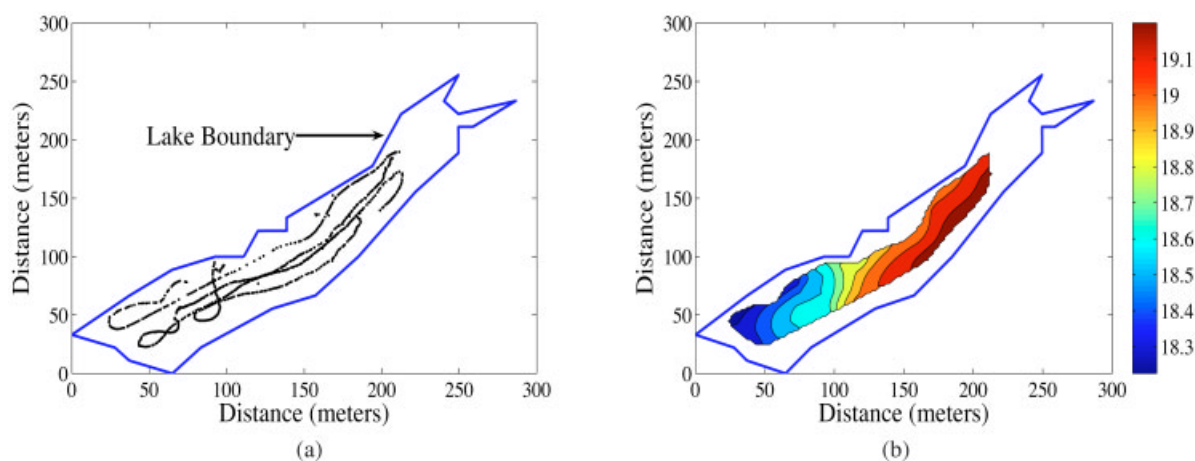


**Figure 10.** The data set of raster scan with robotic boat from 5 PM to 6 PM on May 11, 2006. (a) Observation locations during a scan of NAMOS boat. (b) Temperature distribution at the lake surface for the corresponding scan.

scans performed by NIMS on August 29, 2006 is shown in Figures 11(a) and 11(b). Figures 11(c) and 11(d) show the standard deviation of temperature and dissolved oxygen, respectively, at the corresponding locations. These results conform to the known understanding about stratification of dissolved oxygen and temperature in the lake environment. Figures 11(e) and 11(f) show the variation of temperature and dissolved oxygen as sampled during the four raster scans performed during the August campaign at  $x=32$ . A uniform distribution of temperature is observed from the depth of 1.5 m up to approximately the depth level of 3.5 m. This further conforms to the low standard deviation in temperature distribution observed in this region, as demonstrated in Figure 11(c).

Further, it can be observed from Figures 9(c) and 9(d) that temperature at depths exceeding 1.5 m show a similar pattern during the deployments in both May and June, with little difference between the minimum and the maximum recorded temperatures at a given depth throughout the day. However, there was considerable difference in the observed temperature values with depth even in the middle layer of 1.5 m to 3.5 m, signifying increased stratification in temperature during this season.

#### 4.3.1. Adaptive Sampling

Raster scan experiments during the campaign in August were interspersed with several adaptive experi-

ments during the course of three days. These experiments were motivated by the analysis from the previous two deployments and were planned to selectively sample at a few locations of interest, reducing the sampling time by orders of magnitude.

Based on our discussion with the biologists, we found that thermal stratification, discussed in Section 4.3., along with the optimal light and nutrient concentration (Figure 1), was responsible for subsurface growth of phytoplankton. The temperature gradient across different strata of the lake prevents mixing of water across the gradient, resulting in the biomass distribution getting locked in the middle layer of uniform temperature with thermal gradient above and below it. To characterize the amount of biomass distribution in this middle stratum of uniform temperature, we designed an adaptive experiment to decide sampling locations based on the curvature of thermal gradient. Resulting sampling locations along the depth are sampled at three different locations along the cross section ( $x=16$ , 24, and 32 m). We performed simulations to characterize the effectiveness of sampling based on such an approach. Figure 12(a) represents the subset of the distribution of fluorometry data from  $x=6$  to  $x=34$ . With sampling density of 2 m along the  $x$ -axis, points along the  $y$ -axis were chosen based on the thermal gradient. This resulted in only 165 sampling locations out of a total of 330 sampling locations in

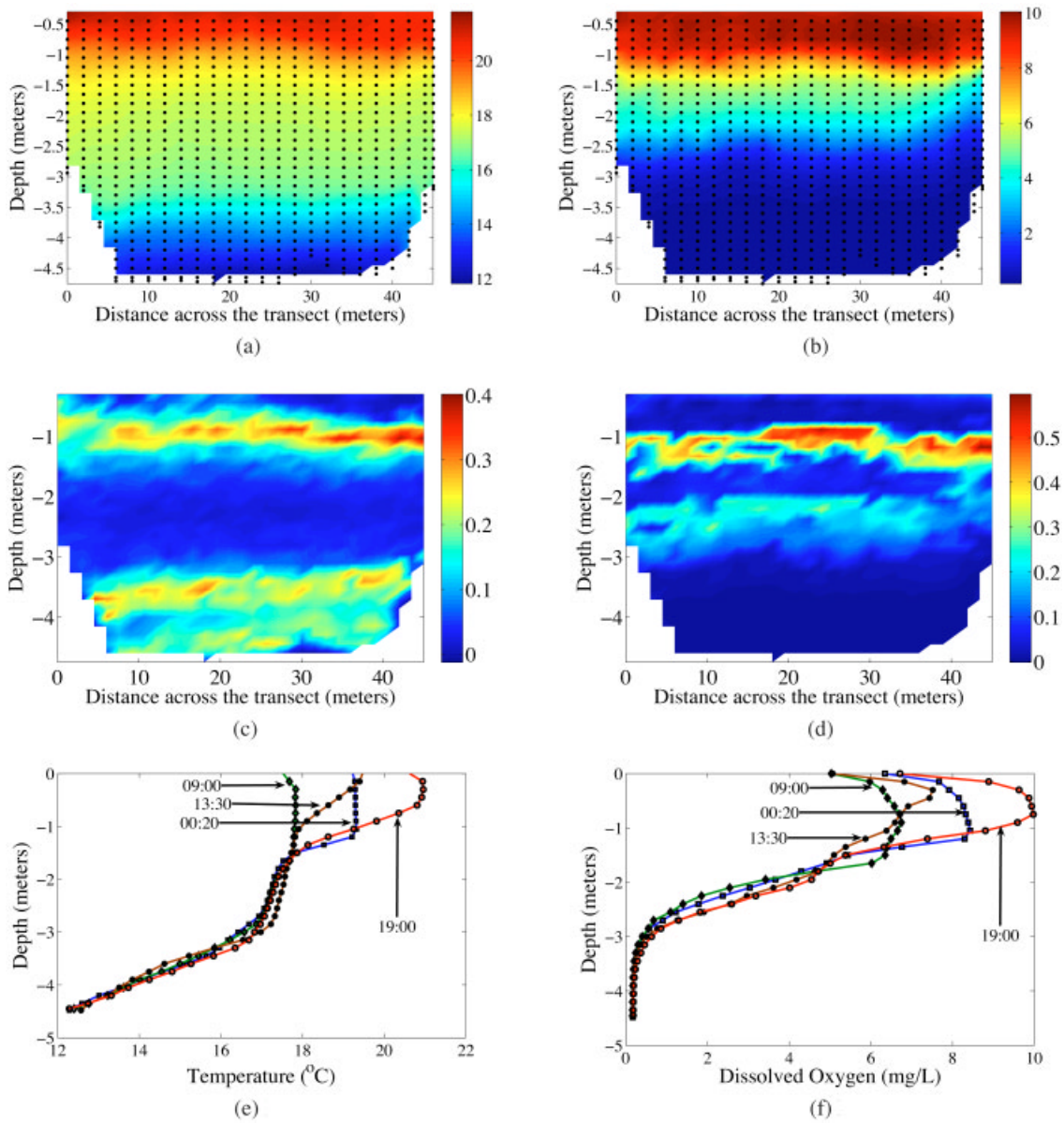


**Figure 11.** Distribution of temperature ( $^{\circ}\text{C}$ ) and dissolved oxygen ( $\text{mg/L}$ ) as observed using NIMS. Spatial distributions and standard deviations correspond to the raster scan performed on August 29, 2006 from 16:49 to 19:47. Distributions at  $x=32$  correspond to data from the four raster scans during the deployment in August. (a) Spatial distribution of temperature ( $^{\circ}\text{C}$ ). (b) Spatial distribution of dissolved oxygen ( $\text{mg/L}$ ). (c) Standard deviation for temperature ( $^{\circ}\text{C}$ ). (d) Standard deviation for dissolved oxygen ( $\text{mg/L}$ ). (e) Distribution at  $x=32$  for temperature. (f) Distribution at  $x=32$  for dissolved oxygen.

the complete subset. Points in Figure 12(a) represent the sampling locations selected using this approach. Local polynomial fit was performed over the data from these locations to create a complete surface dis-

tribution. Figure 12(b) represents a surface of predicted values using the local polynomial fit. As can be observed, the predicted surface distribution is similar to the actual surface distribution shown in

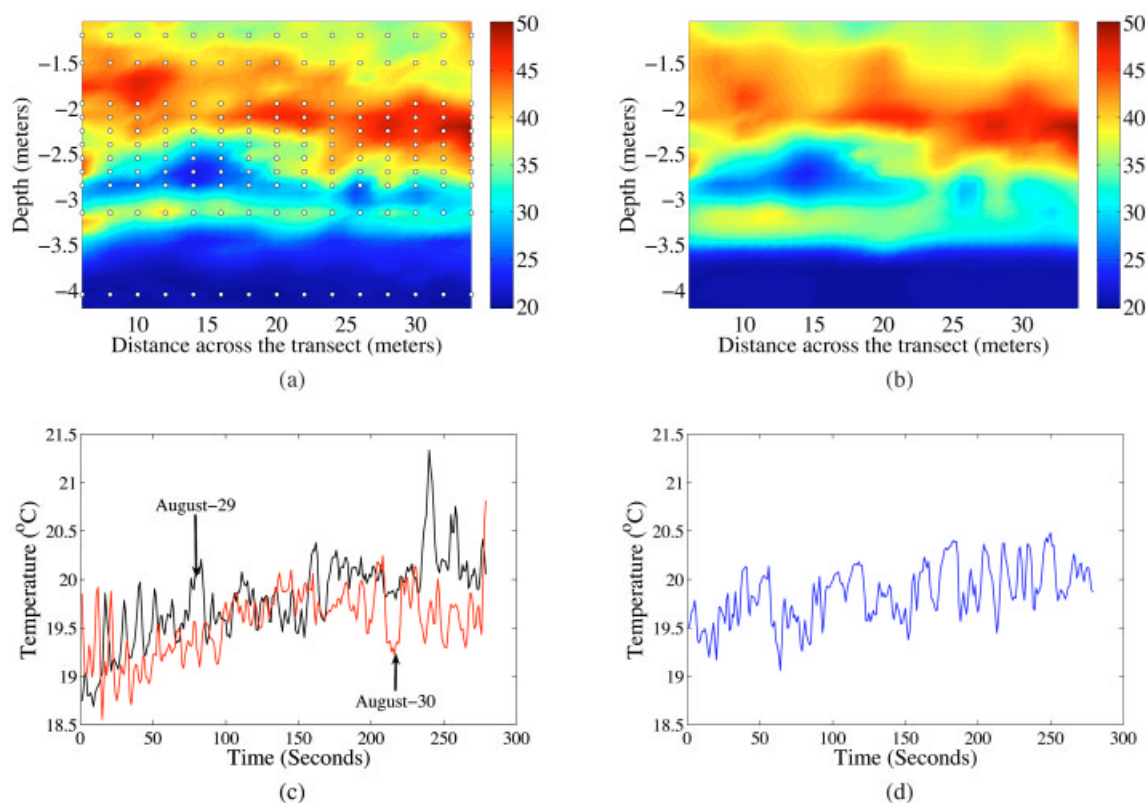


**Figure 12.** Subset of the adaptive experiments performed during the August deployment. Points in Part (a) represent sampling locations selected based on thermal gradient. (a) Subset of surface distribution of chlorophyll (micrograms per liter) as observed by the fluorometer. Points represent observation locations for the adaptive experiment. (b) Surface distribution of chlorophyll (micrograms per liter) after local polynomial fit with sampling based on thermal gradient. (c) Temperature data from thermistor at depth 0.15 m during days when NIMS was not observing in vicinity. (d) Temperature data from thermistor at depth 0.15 m on August 31, when NIMS was observing in vicinity.

Figure 12(a). The total RMS error between the predicted and the actual surface was 4.89 mcg/l.

We designed two experiments to find out if NIMS is causing any interference in the sampled environment by mixing the water from different strata during its vertical motion. In the first experiment, we placed a static buoy very close to the vertical plane observed by NIMS to observe the sudden variations in sampled phenomena, when NIMS is sampling in the vicinity. Figure 12(c) shows the temperature data from the thermistor at a depth of 0.15 m from a buoy, placed close to the NIMS transect for August 29 and 30 from 12:50–13:36. During these two days, NIMS was not making any observations in the vicinity. Figure 12(d) shows the corresponding data during the same time as collected

on August 31. On this day, NIMS was making observations in the vicinity ( $x=24$  to  $x=34$  during this period, when the buoy was located at  $x=30$ ). A preliminary statistical analysis of the relationship between NIMS shuttle position and the nearest buoy showed no significant effects due to churn. This can also be observed by comparing Figure 12(c) and Figure 12(d), that display insignificant variations in observed temperature data by the buoy. In the second experiment, instead of sampling at two nearby locations along the cross section, we alternatively sampled at two locations far away, i.e., instead of sampling at 12, 14, 16, 18 m, etc. along the cross section as in a regular scan, we sampled at 12, 24, 14, 26 m, etc. to reduce the interference in the environment caused by NIMS node and compare the results

with a regular scan. An insignificant difference is observed when the data from the two scans are compared.

#### 4.4. Enhanced Biological Understanding from Robotic Approaches

The unique combination of static and mobile sensor platforms employed in this study (NAMOS providing high-resolution temporal measurements and surface coverage; NIMS providing high-resolution vertical cross sections of the lake) provided unprecedented coverage of fine-scale spatial distributions of phytoplankton biomass in conjunction with observed chemical/physical parameters. This ability to acquire very fine-scale spatial and temporal resolution in the distribution of phytoplankton biomass in conjunction with chemical/physical measurements, has provided unique insights regarding the interplay between the physical, chemical, and biological features driving the distributions and activities of the phytoplankton in Lake Fulmor.

For example, significant diel oscillations in phytoplankton biomass were observed at a fixed depth in the water column of Lake Fulmor. These oscillations were suspected to be the result of a massive diel vertical migration of the phytoplankton community. However, examination of the diel pattern of thermal stratification and mixing, coupled with measurements of chlorophyll fluorescence, indicated that much of the fluctuation observed in the chlorophyll signal might be the result of water stratification or destratification during the day rather than active motility of the phytoplankton [comparing Figures 9(a) and 9(b) note that the regularly spaced “spikes” in chlorophyll fluorescence coincide with the destratification of the water column in the afternoon and evening].

This observed pattern was further confirmed through a more accurate appraisal of the vertical movement of the phytoplankton community using NIMS profiles performed during the day and night [Figures 9(c) and 9(d)]. These profiles revealed that a section of the phytoplankton community did undergo diel vertical migration, but also that this behavior did not include the entire phytoplankton community as initially concluded from the fluorometric measurements at a single depth. Thus, both physical processes (water stratification or destratification) and biological processes (diel vertical migration) contributed to the distribution of phytoplank-

ton biomass vertically in the lake. This level of characterization and understanding would not have been possible without the combined robotic approaches employed in this campaign. The collective information enabled the development of hypotheses regarding the photophysiology of the phytoplankton (due to changing light intensity during the stratification or destratification process) and nutrient acquisition by the population that is vertically migrating. Finally, the collection of physical samples of water enabled the collection of discrete populations of the biological community with which to test these hypotheses.

## 5. RELATED WORK

Despite their highly dynamic nature, aquatic ecosystems have traditionally been sampled sparsely in both time and space. A survey of 52 papers chosen randomly from the journal *Ecology* was performed (Porter et al., 2005) that illustrated that most ecological sampling is either conducted at a small spatial resolution or consists of infrequent or one time sampling without accounting for the spatial and temporal dynamics. This can primarily be attributed to the lack of available technology for sampling at a larger resolution.

Over the last few years, with the development of various robotic platforms, several prototype sensing systems have been used for sensing the aquatic systems at different scales. Individual sensors for spot measurements of phenomena like dissolved oxygen, temperature, specific conductance, pH and others, had been used for characterizing ecosystem metabolism in a mediterranean shallow lake (Lopez-Archilla et al., 2004). Shallow lakes, like Lake Fulmor, with maximum depth around a few meters and negligible water flow, provide a perfect environment that can be observed using a small set of statically deployed sensors to perform a focused study of phytoplankton composition and abundance and the relationship between phytoplankton communities and nutrient dynamics. Buoyed or moored deployment platforms had been used in river environments to provide vertical profiling capabilities over long time periods at key locations (Reynolds-Fleming, Fleming & Luettich 2004). Such systems are ideal for water quality monitoring programs in shallow estuaries where the physical, chemical, and biological characteristics of the observed environment change in response to

external forcing due to the tides, winds, and/or freshwater discharge. They provide the required frequent profiles of hydrographic, chemical, and biological parameters measured in situ. Such systems and experiments, even though they fill in the gap for time sampling continuum in ways that were not feasible earlier, still lack the capability to characterize ecological variability in space.

A remote underwater sampling station is a robotic buoy platform.<sup>9</sup> It consists of a floating platform containing solar panels and sensor package that floats freely below the platform with the capability to sample at user-specified intervals up to 100 m with a precision down to 0.2 m of a target depth. The system, however, lacks the option of real-time data streaming to a remote machine. This system has been used in several studies for characterizing the metabolic rate activities in lake environments (Gelda & Effler, 2002b; Gelda & Effler, 2002a; Popa et al., 2004). This provides additional capability of one dimensional characterization (along the depth) at high spatial resolution.

Autonomous underwater vehicles (AUVs) have been used extensively by the oceanographic community, and more recently in lakes and large rivers (Blidberg, 2001; Kumagai, Ura, Kuroda & Walker, 2002). These are primarily suited for environments with large spatial coverage and for observing phenomena where dense sampling, up to an order of a few meters, is not required. As an example, Tantan, an AUV developed by Kumagai et al., 2002 is 2.0 m long, 0.75 m wide, and 0.75 m high and weighs 180 kg. It is used for monitoring a lake with a surface area of 670 km<sup>2</sup> and a depth of 41 m. Additionally, with the currently available technology, AUVs provide very little control of the system to the user as it performs its task. With minimal real-time control over the system, it is difficult to implement any closed-loop approach (where the next set of observation locations depend on data observed at already visited set of locations) or real-time adaptive approach with the system.

The need for large-scale experiments for characterizing the response of ecosystems has long been pressed for (Carpenter, 1998). The use of multidisciplinary teams for implementation and rapid, successful deployment has been demonstrated in the North Temperate Lakes Long Term Ecological Project (Kratz et al., 2003). A literature survey conducted by our re-

search team reveals that for the first time an autonomous robotic system, along with the static buoys, has been successfully deployed to gather data with high spatial and temporal resolution mapping in a representative lake environment.

## 6. CONCLUSIONS AND FUTURE WORK

In this paper we described a human-assisted robotic team campaign for phytoplankton study at a representative subalpine lake, Lake Fulmor, in the San Jacinto Mountain Reserve. The robotic team consisted of the NAMOS system and NIMS, allowing high precision autonomous sampling of a lake cross section with onboard sensors. Each system is equipped with sensors for observing several variables that can be correlated with the growth of phytoplankton in a lake environment.

Constant software and hardware maintenance of the system, along with its recalibration, is required for any such environmental field campaign to ensure high position precision and robustness of operation. Additionally, in such a campaign, in-field data analysis is required to iteratively improve the experimental design. The success of such a campaign critically depends on the quality of the collected data. This requires robustness in hardware and detection of failures as soon as possible such that a problem resolution can be applied immediately. Robustness of our system was achieved in both the hardware and in data collection by redundancy in sensing payloads (two similar sensor package modules), real-time data access and analysis, temporal and spatial experiment variations, and studying the effects of the mobile system motion on the quality of collected data. Redundancy in sensing payloads proved to be invaluable, since sensor failure to provide or log data was indeed observed in one experimental phase. Experimental results were not lost, however, since data were successfully recovered from a second redundant device. The real-time data access allowed us to monitor physically, as well as in software, the real-time data stream from the sensors deployed on the mobile robot.

We performed an iterative experiment design approach, deciding the next set of experiments based on prior knowledge and observations from previous experiments to perform detailed three-dimensional characterization of the observed phenomena. For this purpose, high spatial resolution raster scans were

<sup>9</sup>Developed by Apprise Technologies.

performed using NIMS to characterize the spatial distribution of the observed phenomena along the selected cross section, discounting for the temporal variation. The statically distributed buoy system, along with repeated raster scans, were used to characterize the temporal distribution at different scales. We also performed several experiments that verified minimal effects of the mobile system on the phenomena distribution (due to its vertical motion inside the water) and that the disturbance of the environment introduced by the system was insignificant.

Interspersed with these experiments, we also performed a set of adaptive experiments, performing sampling only in the regions with high variability. We used field reconstruction from the previous deployments of the robotic system to identify areas of high interest and then focused the sampling only in those regions. This approach reduced the sampling time significantly. It also confirms that once the spatiotemporal dynamics of the phenomena distribution is characterized, an experiment design can be biased to perform adaptive sampling, thus reducing the total sampling time and hence enabling the spatial characterization at a larger scale.

Finally, we performed a set of remotely triggered water sample collection (physical sampling) experiments that revealed interesting results about the change in microbial community over the course of several months. In addition, physical sampling allowed performing detailed lab analysis for the parameters that cannot be detected with the currently available in-field sensors.

The robotic approach employed in this study allowed unique insights into phytoplankton community structure and dynamics. Due to the numerous temporal and spatial scales that affect phytoplankton dynamics, however, even this enhanced capability must entail compromises or tradeoffs that take into account the specific goals of the biological study, and how robotics can best meet these goals on the budget available. This decision, rather than specific limitations of the robotic approach, must drive the design of the instrumentation or the robotic systems. The relatively small size of Lake Fulmor and the magnitude of our campaign enabled a “systems-level” approach for this study. The combined use of the static node and autonomous surface vehicle (NAMOS) with high spatial or vertical profiling capability (NIMS) provided a characterization of the small-scale temporal (minutes) and spatial (centimeter) distributions of the phytoplankton community throughout

much of the lake. Such a systems-level approach in most of the aquatic environments must make clear decisions of the questions that can be addressed, and the scales of measurement that need to be investigated.

In the future we plan to exploit the experience obtained in the lake deployment to the implementation of autonomous environmental observatories. In such systems, the collaboration of static and mobile systems can yield unprecedented results by capturing the phenomena of interest (high fluorescence areas potentially indicating areas of high phytoplankton activity) accurately in space and in time.

## ACKNOWLEDGMENTS

This material is based upon work supported in part by the U.S. National Science Foundation (NSF) (Grant Nos. ANI-00331481, DDDAS-0540420, CCR-0120778, CAREER-0133947) and National Oceanic and Atmospheric Administration (NOAA) (Grant No. MERHAB-NA05NOS4781228.). Any opinions, findings, and conclusions or recommendations expressed in this material are those of the authors and do not necessarily reflect the views of the NSF and NOAA. We are also thankful to our reviewers for providing their invaluable comments that significantly improved the content and presentation of the paper.

## REFERENCES

- Blidberg, D.R. (May, 2001). The development of autonomous underwater vehicles (AUVs); A brief summary. In IEEE Int. Conf. Robotics and Automation, Seoul, Korea.
- Carpenter, S. (1998). Need for large scale experiments to assess and predict the response of ecosystems to perturbation. In *Successes, limitations and frontiers in ecosystem science.*, New York.
- Gelda, R., & Effler, S. (2002a). Estimating oxygen exchange across the air-water interface of a hypereutrophic lake. *Hydrobiologia*, 487, 243–254.
- Gelda, R., & Effler, S. (2002b). Metabolic rate estimates for a eutrophic lake from diel dissolved oxygen signals. *Hydrobiologia* 485(16), 51–66.
- Girod, L., Elson, J., Cerpa, A., Stathopoulos, T., Ramanathan, N., & Estrin, D. (2004). Emstar: A software environment for developing and deploying wireless sensor networks. In *Proceedings of the 2004 USENIX Technical Conference*, Boston, MA.
- Harmon, T.C., Ambrose, R.F., Gilbert, R.M., Fisher, J.C.,

- Stealey, M., & Kaiser, W.J. (2006). High resolution river hydraulic and water quality characterization using rapidly deployable networked infomechanical systems (NIMS RD). *Environ. Eng. Sci.* 24(2), 151–159.
- James San Jacinto Mountain Reserve (2006). <http://www.jamesreserve.edu>.
- Jordan, B., Batalin, M., & Kaiser, W. (2007). NIMS RD: A rapidly deployable cable based robot. In *IEEE Int. Conf. Robots and Automation*, pp. 144–150, Rome, Italy.
- Kratz, T., Deegan, L., Harmon, M., & Lauenroth, W. (2003). Ecological variability in space and time: Insights gained from the US LTER program. *BioScience*, 53(11), 57–67.
- Kumagai, M., Ura, T., Kuroda, Y., & Walker, R. (2002). A new autonomous underwater vehicle designed for lake environment monitoring. *Adv. Rob.*, 16, 17–26.
- Lopez-Archilla, A., Molla, S., Coletto, M., Guerrero, M., & Montes, C. (2004). Ecosystem metabolism in a mediterranean shallow lake (Laguna de Santa Olalla, Doñana national park, SW Spain). *Wetlands*, 24(4), 848–858.
- Pon, R., Batalin, M., Gordon, J., Rahimi, M., Kaiser, W., Sukhatme, G., Srivastava, M., & Estrin, D. (2005). Networked infomechanical systems: A mobile wireless sensor network platform. In *Int. Conf. Information Processing in Sensor Networks*, 2005, pp. 376–381.
- Popa, D., Sanderson, A., Komerska, R., Mupparapu, S., Blidberg, D., & Chappel, S. (2004). Adaptive sampling algorithms for multiple autonomous underwater vehicles. In *Autonomous Underwater Vehicles*, 2004 IEEE/OES, pp. 108–118.
- Porter, J., Arzberger, P., Braun, H.-W., Bryant, P., Gage, S., Hansen, T., Hanson, P., Lin, C.-C., Lin, F.-P., Kratz, T., Michener, W., Shapiro, S., & Williams, T. (2005). Wireless sensor networks for ecology. *BioScience*, 55(12), 561–572.
- Reynolds-Fleming, J.V., Fleming, J.G., & Luettich, R.A. (2004). Portable autonomous vertical profiler for estuarine applications. *Estuaries*, 25, 142–147.
- Singh, A., Batalin, M.A., Chen, V., Stealey, M., Jordan, B., Fisher, J.C., Harmon, T.C., Hansen, M.H., & Kaiser, W.J. (2007a). Autonomous robotic sensing experiments at San Joaquin River. In *IEEE Int. Conf. Robots and Automation*, pp. 4987–4993, Rome, Italy.
- Singh, A., Batalin, M.A., Stealey, M., Chen, V., Hansen, M.H., Harmon, T.C., Sukhatme, G.S., & Kaiser, W.J. (2007b). Mobile robot sensing for environmental applications. In *6th Int. Conf. Field and Service Robots*, Chamonix, France.
- Sukhatme, G.S., Dhariwal, A., Zhang, B., Oberg, C., Stauffer, B., & Caron, D.A. (2006). The design and development of a wireless robotic networked aquatic microbial observing system. *Environ. Eng. Sci.*, 24(2), 205–215.